

Article

Separation of Benzene and Cyclohexane Using Eutectic Solvents with Aromatic Structure

Mohamed K. Hadj-Kali ^{1,*}, M. Zulhaziman M. Salleh ^{2,*}, Irfan Wazeer ¹, Ahmad Alhadid ³ and Sarwono Mulyono ¹

¹ Chemical Engineering Department, King Saud University, Riyadh 11421, Saudi Arabia; iwazeer@ksu.edu.sa (I.W.); sarmulyoprayitno@ksu.edu.sa (S.M.)

² Department of Chemical and Process Engineering, Faculty of Engineering and Built Environment, Universiti Kebangsaan Malaysia, Bangi 43600, Malaysia

³ Biothermodynamics, TUM School of Life Sciences, Technical University of Munich, Maximus-von-Imhof-Forum 2, 85354 Freising, Germany; ahmad.alhadid@tum.de

* Correspondence: mhadjkali@ksu.edu.sa (M.K.H.-K.); zulhaziman@ukm.edu.my (M.Z.M.S.)

Abstract: The separation of benzene and cyclohexane is a challenging process in the petrochemical industry, mainly because of their close boiling points. Extractive separation of the benzene-cyclohexane mixture has been shown to be feasible, but it is important to find solvents with good extractive performance. In this work, 23 eutectic solvents (ESs) containing aromatic components were screened using the predictive COSMO-RS and their respective performance was compared with other solvents. The screening results were validated with experimental work in which the liquid–liquid equilibria of the three preselected ESs were studied with benzene and cyclohexane at 298.5 K and 101.325 kPa, with benzene concentrations in the feed ranging from 10 to 60 wt%. The performance of the ESs studied was compared with organic solvents, ionic liquids, and other ESs reported in the literature. This work demonstrates the potential for improved extractive separation of the benzene-cyclohexane mixture by using ESs with aromatic moieties.

Keywords: ionic liquids; eutectic solvents; benzene; cyclohexane; LLE; COSMO-RS



Citation: Hadj-Kali, M.K.; Salleh, M.Z.M.; Wazeer, I.; Alhadid, A.; Mulyono, S. Separation of Benzene and Cyclohexane Using Eutectic Solvents with Aromatic Structure. *Molecules* **2022**, *27*, 4041. <https://doi.org/10.3390/molecules27134041>

Academic Editors: Zhijian Tan, Hongye Cheng and Baokun Tang

Received: 6 May 2022

Accepted: 20 June 2022

Published: 23 June 2022

Publisher's Note: MDPI stays neutral with regard to jurisdictional claims in published maps and institutional affiliations.



Copyright: © 2022 by the authors. Licensee MDPI, Basel, Switzerland. This article is an open access article distributed under the terms and conditions of the Creative Commons Attribution (CC BY) license (<https://creativecommons.org/licenses/by/> 4.0/).

1. Introduction

The separation of aromatic-aliphatic hydrocarbon mixtures is a challenging process in downstream fuel processing. An ordinary distillation method is economically unviable because the two compounds often have boiling points close to each other, i.e., 80.1 °C for benzene and 80.74 °C for cyclohexane. Furthermore, the formation of azeotropes in some combinations leads to additional difficulties in process efficiency. This suggests the use of more advanced separation techniques, which are classified into three types [1,2]: liquid extraction (for 20–65% aromatics content), extractive distillation (for 65–90% aromatics content), and azeotropic distillation (for more than 90% aromatics content). The most commonly used solvents in these processes are conventional organic compounds, such as sulfolane, polyethylene glycols, tetraethylene glycol, di-methyl sulfoxide, N-methylpyrrolidone, and N-formylmorpholidone [2]. Despite their industrial use, the use of these solvents suffers from high energy consumption, high capital and operating costs, and process complexity [3]. Moreover, there is no feasible process for the separation of aromatics content below 20%.

Liquid–liquid extraction is an interesting process because it can be operated at ambient conditions. To achieve efficient extraction, the choice of solvent is a crucial step, as it should be chemically stable, non-corrosive, inexpensive and easy to obtain. Interestingly, ionic liquids (ILs) have been extensively researched for their potential use as alternative solvents in many applications. In addition to their chemical and thermal stability, ILs also possess particular advantages over conventional industrial solvents, especially due to their

negligible vapor pressure, wide range, and tunable properties. Moreover, ILs have also shown promising results in the separation of aromatics and aliphatics [4–7].

The feasibility of IL as extraction solvents was usually evaluated based on the benzene distribution ratio and selectivity. Several ILs were reported to show good selectivity, such as 1-ethyl-3-methylimidazolium tetrafluoroborate [$C_2\text{Mim}][\text{BF}_4]$], 1-alkyl-3-methylimidazolium hexafluorophosphate [$C_4\text{mim}][\text{PF}_6]$], and 1-butylpyridinium tetrafluoroborate [$\text{Bpyr}][\text{BF}_4]$] [8,9]. [$C_4\text{mim}][\text{PF}_6]$ remarkably showed extremely high solvent selectivity at low composition (<15%) of benzene in the raffinate phase, suggesting that it is suitable for the deep separation of benzene and cyclohexane [9]. The choice of ILs is not limited to selectivity. For example, [$C_2\text{py}][\text{EtSO}_4]$ was selected due to its ease of preparation, market availability, and satisfactory results in the separation of benzene from its mixture with other aliphatic compounds [10,11]. Although ILs have higher extraction performance than organic solvents, their use is rather limited mainly due to their toxicity and high cost [12].

Eutectic solvents (ESs) have been identified as a promising alternative for many separation applications [13]. ESs have been mainly investigated in the fields of electrodeposition of metals [14], nanotechnology [15], and extraction and separation processes [16,17]. Recently, however, they have also received attention in the fields of solar energy [18,19], photosynthesis [20], and electrochemical sensing [21]. Some examples of the use of ESs in various applications are listed in Table S1. ESs are widely recognized as a new class of IL analogs because they share many features and properties with ILs, especially that they are liquid at ambient temperature [22,23]. However, ESs can be prepared by simple mixing of inexpensive and natural substances. ESs are eutectic mixtures containing a salt and a hydrogen bond donor, forming a mixture with a much lower melting temperature than the raw materials [24,25].

Although the advantages of ESs are recognized, there is little information on their potential use in the separation of benzene and cyclohexane. In our previous work [26], five ESs were preselected using the Conductor-like Screening Model for Realistic Solvation (COSMO-RS), namely tetrabutylammonium bromide:sulfolane (TBABr:sulf (1:7)), methyl triphenylphosphonium bromide:triethylene glycol (MTPPBr: TEG (1:4)), tetrabutylammonium bromide:triethylene glycol (TBABr: TEG (1:4)), choline chloride:triethylene glycol (ChCl: TEG (1:4)), and methyltriphenylphosphonium bromide:propanediol (MTPPBr: PD (1:4)). The ESs were found to be useful extracting solvents in the separation of benzene-cyclohexane mixtures by liquid–liquid extraction. Although the benzene distribution ratio was low, efficient extraction can be achieved by a multistage process [26]. In another study [27], two ESs, namely tetrabutylammonium bromide:sulfolane, TBABr:sulf (1:5), and trimethylamine hydrochloride:ethylene glycol, TMAHCl: EG (1:5) were selected to separate benzene and cy-clohexane mixtures. Similar to our results, the study showed that TBABr:sulf (1:5) is a promising solvent for the extractive separation of the benzene-cyclohexane mixture.

In liquid–liquid extraction, it is ideal to use an extraction solvent that achieves high values in both selectivity and distribution ratio. However, numerous reports have found that in most cases, the distribution ratio of an extraction solvent has an inverse relationship with selectivity. This relationship presents a clear challenge in finding a solvent with high values for both selectivity and distribution ratio. Therefore, the development and modification of the solvent used is an important task. In summary, three attempts have been made to obtain ILs with high selectivity and high distribution ratio [28]: (1) searching for new and unusual ILs, (2) mixing with green co-solvents, or (3) mixing ILs. Solvent mixing has attracted particular attention in the extractive separation of aromatic and aliphatic compounds and has been discovered as a new efficient and versatile technique to optimize extraction performance [29–32].

COSMO-RS has been widely used in many research computational approaches due to its fast and reliable prediction capability. COSMO-RS combines statistical thermodynamics and quantum chemical calculations to predict the thermodynamic properties of solvents

without using experimental data. Considering this advantage, many screening processes have been performed to help research groups find the best solvents for various applications, such as desulfurization and denitrification. The mathematical derivations for the interaction energies, chemical potential, and activity coefficient derived by the developers of COSMO-RS can be found elsewhere [33,34], and we have summarized the equations involved in our previous work [35–37]. COSMO-RS has been used for various thermodynamic predictions and validations in critical processes such as denitrification [38], desulfurization [39,40], and separation of aromatic and aliphatic mixtures [41–43]. In this work, the extraction performance of ESs with aromatic structure for the separation of benzene and cyclohexane mixtures was investigated using COSMO-RS screening and validation by experimental liquid–liquid extraction.

2. Results and Discussion

2.1. COSMO-RS Screening Results

In this study, COSMO-RS was used to screen the appropriate ESs by calculating their capacity (C_{∞}), selectivity (S_{∞}), and performance index (PI_{∞}) at infinite dilution. The results of the ES screening are shown in Figures 1–3. In these Figures, the studied ESs were sorted in descending order by the value of capacity at infinite dilution (C_{∞}), since solvent capacity has been reported to have a much greater impact on production cost than selectivity. As seen in Figure 1, two ESs with different hydrogen bonding acceptors showed high C_{∞} values, namely BTMACl:PTSA (3:7) and ATPPBr:PTSA (1:3). In addition, a general trend was also observed for some ESs. TMGly generally showed a higher C_{∞} value compared to ChCl. The capacity of ESs generally increases with longer cation alkyl chain, i.e., TBABr:PTSA (1:2) > TEABr:PTSA (1:2) and TBACl:PTSA (1:2) > TEACl:PTSA (1:2).

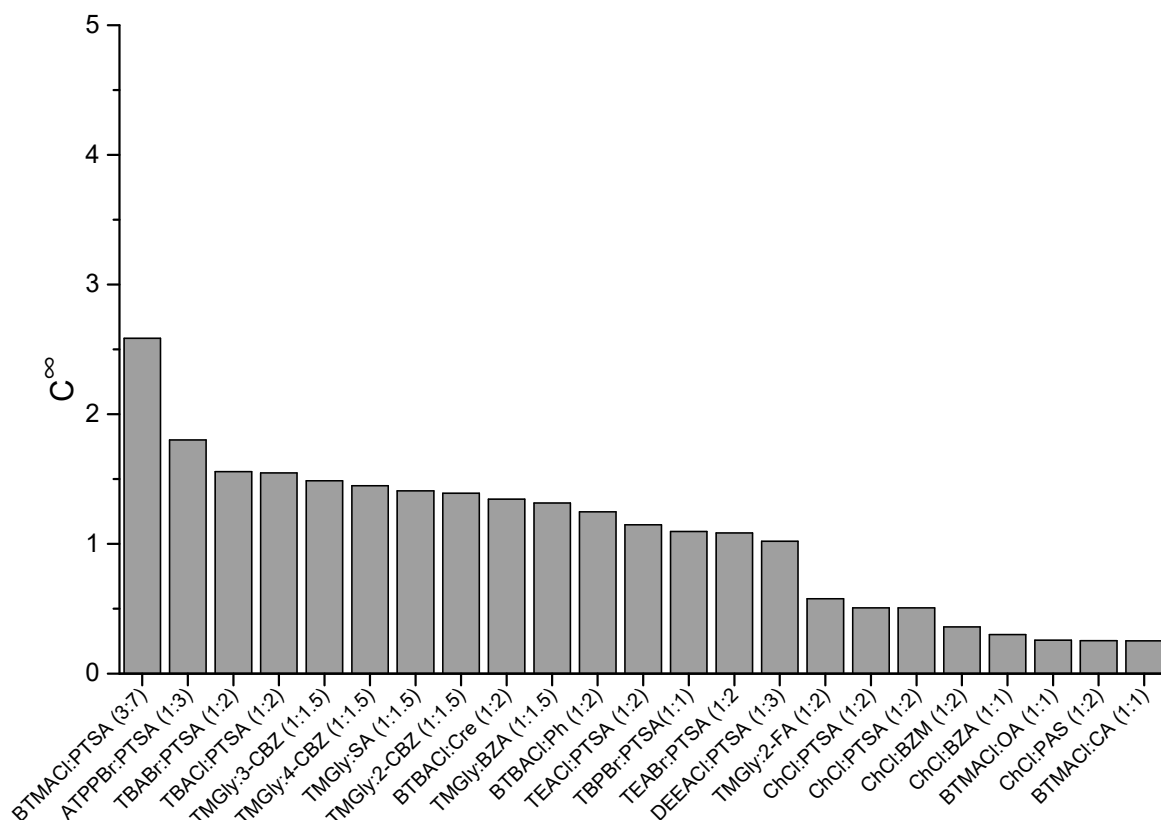


Figure 1. Capacity of ESs at infinite dilution.

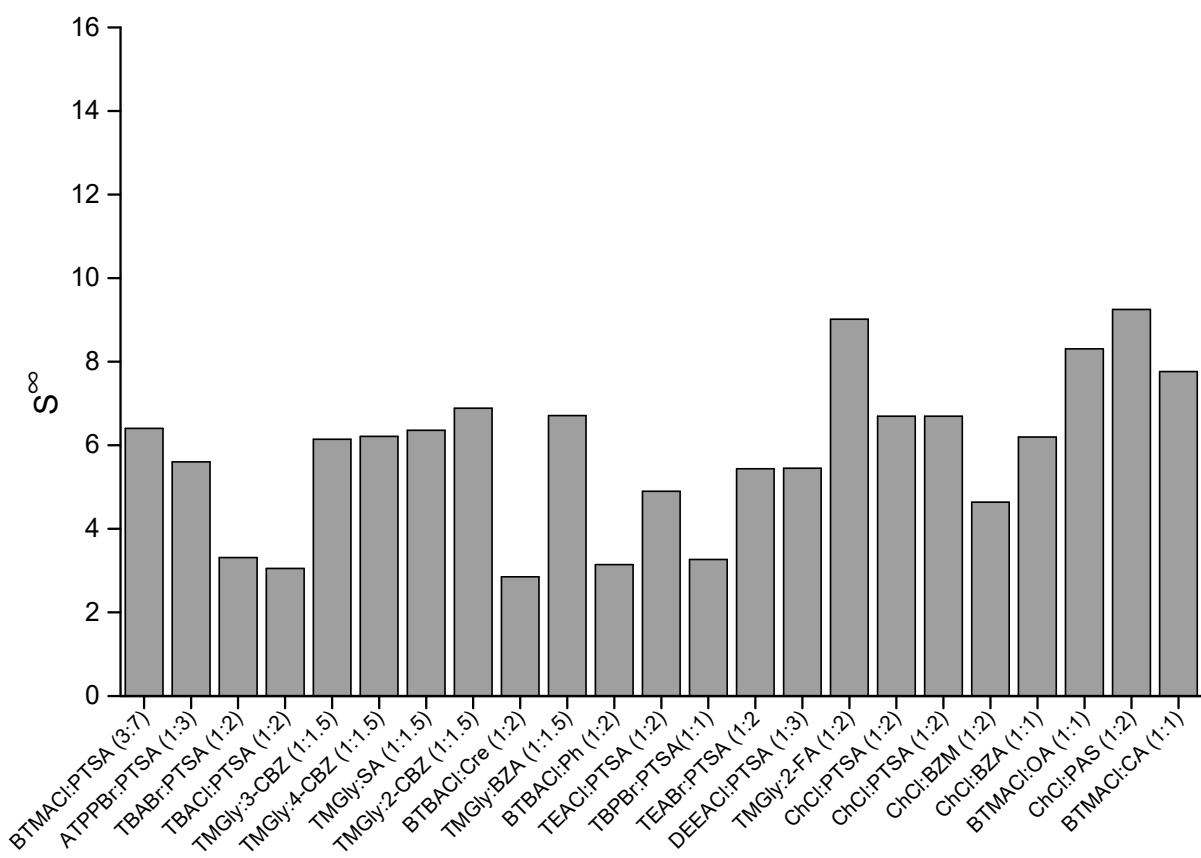


Figure 2. Selectivity of ESs at infinite dilution.

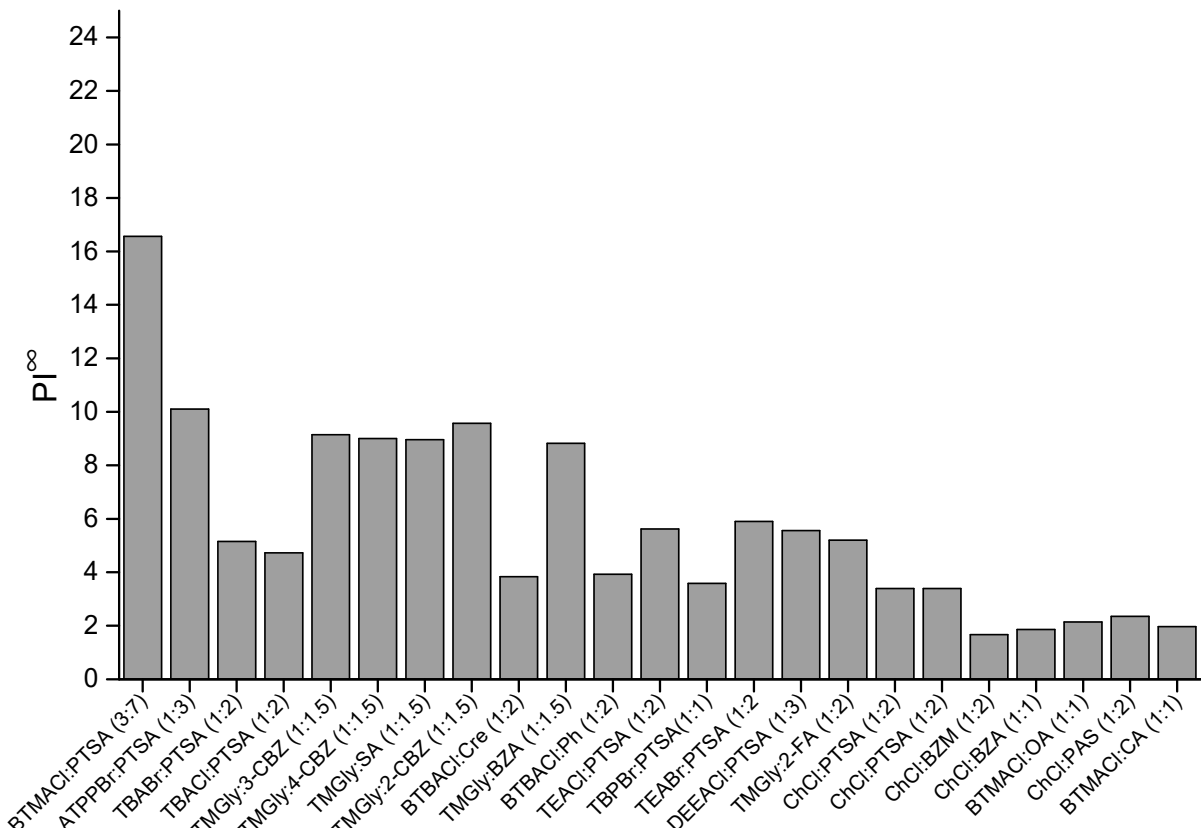


Figure 3. Performance index of ESs at infinite dilution.

As seen in Figure 2, the five ESs with the highest selectivity are in the order, $\text{ChCl: PAS (1:2)} > \text{TMGly:2-FA (1:2)} > \text{BTMACl:OA (1:1)} > \text{BTMACl: CA (1:1)} > \text{TMGly:2-CBZ (1:1.5)}$. An inverse trend was generally observed when evaluating the capacity and selectivity of the same ESs. The capacity of an ES reflects its ability to extract other components regardless of their specific structure. On the other hand, selectivity evaluates the efficiency of the solvent in extracting the specific solute (benzene in this work). The predicted selectivity of the ESs in this work is generally higher than that of the ESs screened in our previous work [26], where the average selectivity increment is around 10.5%. This indicates the significant influence of the aromatic group on the selectivity. From this result, it can be concluded that the presence of an aromatic ring in the ES structure could enhance the selective interaction between ES and benzene through π - π stacking.

The performance index combines both selectivity and capacity by simple multiplication. Thus, the PI_{∞} is a mathematical operation that evaluates overall extraction performance by considering the inverse relationship between C_{∞} and S_{∞} . As seen in Figure 3, five ESs with the highest PI_{∞} were in the order of $\text{BTMACl:PTSA (3:7)} > \text{ATPPBr:PTSA (1:3)} > \text{TMGly:2-CBZ (1:1.5)} > \text{TMGly:3-CBZ (1:1.5)} > \text{TMGly:4-CBZ (1:1.5)}$. In liquid–liquid extraction, capacity indicates the amount of solvent required, while selectivity evaluates extraction efficiency. An ideal extraction solvent for efficient extraction would have high capacity and selectivity. However, due to inverse proportionality, it is difficult to obtain ESs with high values for both capacity and selectivity. Therefore, there is a conflict with one of these properties in the solvent screening process. Based on the results from COSMO-RS, BTMACl:PTSA (3:7) is expected to be the best extraction solvent because it has the highest value for both C_{∞} and PI_{∞} .

2.2. Experimental Selectivity and Distribution Ratio

In this work, experimental LLE was performed for the ESs obtained by mixing BTBACl with phenol or cresol in a molar ratio of 1:2 and for another ES, formed by mixing TBPP with PTSA in a molar ratio of 1:1. The LLE data at 298.15 K and 101.325 kPa were used to investigate the efficiency of benzene extraction from a benzene-cyclohexane mixture using the proposed aromatic-based ESs as extractants. The hydrocarbon-rich phase was analyzed by ^1H NMR spectroscopy, and no ES constituents were detected. Accordingly, the two-phase system was assumed as a pseudo-ternary system, where the ES ratio remains constant. In this context, the efficiency of the extracting solvents was evaluated based on two important parameters: selectivity (S) and distribution ratio (D). Equations (1)–(3) were used to calculate the selectivity and the distribution ratio [26,44]:

$$D_{\text{Ben}} = x_{\text{Ben}}^{\text{B}} / x_{\text{Ben}}^{\text{T}} \quad (1)$$

$$D_{\text{Ch}} = x_{\text{Ch}}^{\text{B}} / x_{\text{Ch}}^{\text{T}} \quad (2)$$

$$S = \frac{D_{\text{Ben}}}{D_{\text{Ch}}} = x_{\text{Ben}}^{\text{B}} / x_{\text{Ben}}^{\text{T}} \times x_{\text{Ch}}^{\text{T}} / x_{\text{Ch}}^{\text{B}} \quad (3)$$

where x is the concentration in mole fraction, Ben stands for benzene, and Ch for cyclohexane. Superscripts B and T refer to the bottom and top phases, respectively.

The LLE data along with the distribution ratio and selectivity of the three systems [benzene + cyclohexane + BTBACl + Ph (1:2, HBA:HBD molar ratio)], [benzene + cyclohexane + BTBACl + Cre (1:2, HBA:HBD molar ratio)], and [benzene + cyclohexane + TBPP + PTSA (1:1, HBA:HBD molar ratio)] are shown in Table 1. x_{HBA} and x_{HBD} represent the molar composition of hydrogen bond acceptor and hydrogen bond donor, respectively. The experimental results of the three systems studied were plotted in ternary diagrams by treating the ESs as a single component in Figure 4 to graphically illustrate the phase equilibria. It can be observed that one pair of the components of all ternary systems exhibits partial miscibility with each other ([BTBACl:Cre or BTBACl:Ph + benzene or cyclohexane]), while the other pair of components exhibits complete miscibility ([benzene + cyclohexane]), i.e., in ternary systems consisting of BTBACl:Cre or BTBACl:Ph + benzene + cyclohex-

ane, the binary compounds BTBACl:Cre or BTBACl:Ph + benzene and BTBACl:Cre or BTBACl:Ph + cyclohexane present partial miscibility, while the binary compound benzene + cyclohexane presents complete miscibility. It is also worth noting that for the first two ESs, i.e., BTBACl:Ph (1:2) and BTBACl:Cre (1:2), high concentrations of cyclohexane were consistently observed in the extract phase. This could be due to the benzyl group of the hydrogen bond acceptor interacting with cyclohexane such as the interactions in the benzene-cyclohexane mixture. The cross-solubility of cyclohexane in the ES phase would not cause much difficulty in the post-extraction system, since the ES can be recycled by heating off the cyclohexane due to the ES negligible vapor pressure.

Table 1. Molar composition of experimental tie-lines, distribution ratio (D), and selectivity (S) data for three systems at 101.325 kPa and T = 298.15 K.

Raffinate Phase		Extract Phase				D _{Ch}	D _{Ben}	S
x _{Ben}	x _{Ch}	x _{Ben}	x _{Ch}	x _{HBA}	x _{HBD}			
Benzene (1) + Cyclohexane (2) + BTBACl (3) + Ph (4) (1:2, HBA:HBD molar ratio)								
0.079	0.921	0.125	0.350	0.175	0.349	0.381	1.588	4.17
0.163	0.837	0.223	0.332	0.148	0.297	0.396	1.370	3.46
0.243	0.757	0.316	0.320	0.121	0.243	0.423	1.301	3.08
0.322	0.678	0.401	0.299	0.100	0.200	0.441	1.245	2.82
0.413	0.587	0.473	0.275	0.084	0.168	0.468	1.144	2.44
Benzene (1) + Cyclohexane (2) + BTBACl (3) + Cre (4) (1:2, HBA:HBD molar ratio)								
0.079	0.921	0.122	0.480	0.133	0.265	0.521	1.547	2.97
0.153	0.847	0.235	0.453	0.104	0.208	0.535	1.542	2.88
0.230	0.770	0.312	0.432	0.085	0.170	0.562	1.356	2.41
0.323	0.677	0.383	0.411	0.069	0.137	0.607	1.187	1.95
Benzene (1) + Cyclohexane (2) + TBPB (3) + PTSA (4) (1:1, HBA:HBD molar ratio)								
0.089	0.911	0.106	0.204	0.345	0.345	0.518	1.191	5.31
0.179	0.821	0.202	0.190	0.304	0.304	0.381	1.130	4.89
0.267	0.733	0.293	0.195	0.256	0.256	0.296	1.095	4.10
0.359	0.641	0.368	0.175	0.229	0.229	0.469	1.023	3.74
0.461	0.539	0.409	0.157	0.217	0.217	0.391	0.888	3.06
0.553	0.447	0.512	0.159	0.165	0.165	0.312	0.926	2.61

Standard uncertainties are: u(T) = 0.1 K, u(P) = 0.1 kPa, u(x) = 0.009.

The distribution coefficients and selectivity using BTBACl:Ph (1:2), BTBACl:Cre (1:2), and TBPB:PTSA (1:1) are shown in Figures 5–7, respectively. It can be observed that the weight fraction of benzene in the feed does not have much effect on the distribution ratio of BTBACl:Ph (1:2) and BTBACl:Cre (1:2), as only a slight change in the distribution ratio was observed at higher benzene concentrations in the feed in both ternary systems. This suggests that the extraction capacity of benzene from benzene-cyclohexane mixtures using BTBACl:Ph (1:2) and BTBACl:Cre (1:2) does not change significantly at different benzene concentrations in the feed. This would open a wide applicability of both ESs as extractants for higher benzene concentrations in the feed. In contrast, when TBPB:PTSA (1:1) was used as the extractant, the distribution ratio was less than one when the benzene concentration in the feed was greater than 40 wt%. This explains the change in the slope of tie lines from positive to negative values in Figure 4c, where the negative slopes indicate a higher amount of benzene in the raffinate phase than in the extract phase. On the other hand, it is observed that all the selectivity values for all the ternary systems are greater than one, indicating the possibility of separation by liquid–liquid extraction.

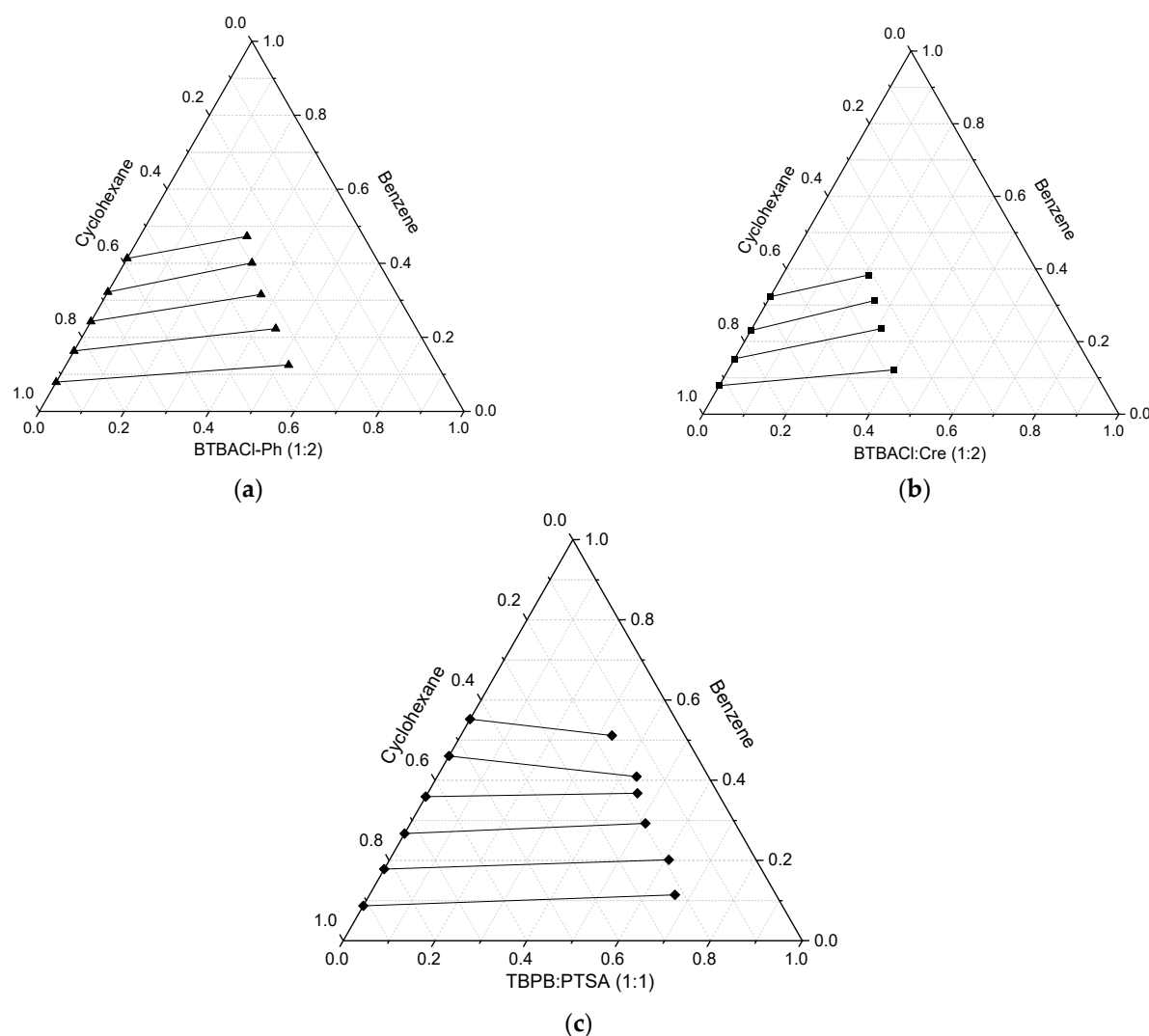


Figure 4. Ternary liquid–liquid equilibria diagrams for (a) BTBACl:Ph (1:2) + benzene + cyclohexane; (b) BTBACl:Cre (1:2) + benzene + cyclohexane and (c) TPBP:PTSA (1:1) + benzene + cyclohexane.

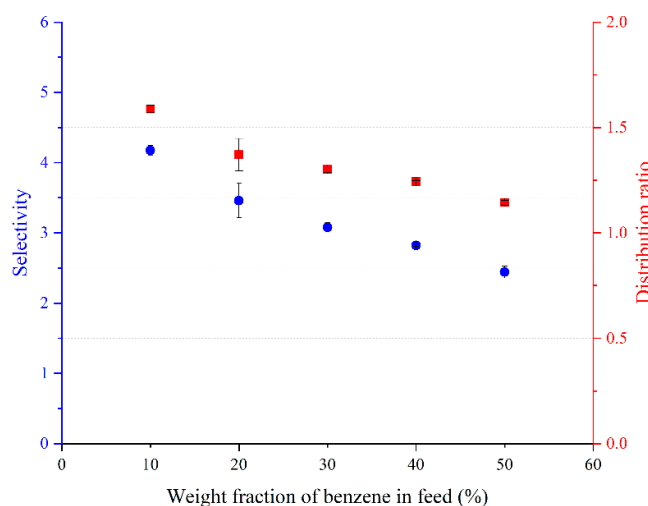


Figure 5. Variation of the distribution ratio and selectivity with benzene weight fraction in the feed for [Benzene (1) + Cyclohexane (2) + BTBACl:Ph (1:2) (3)].

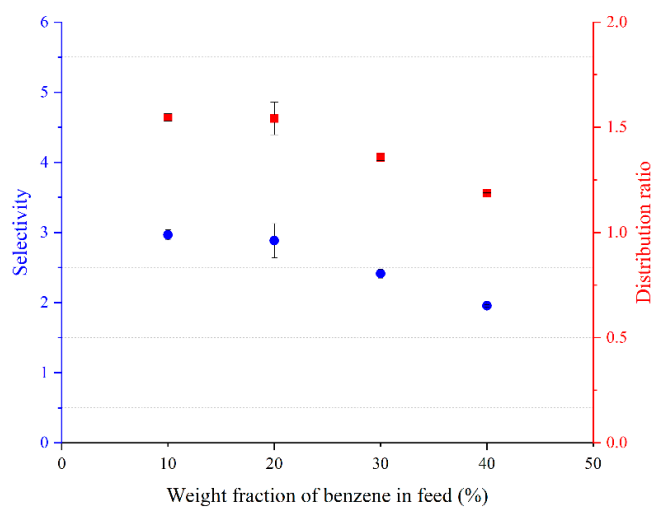


Figure 6. Variation of the distribution ratio and selectivity with benzene weight fraction in the feed for [Benzene (1) + Cyclohexane (2) + BTBAcL:Cre (1:2) (3)].

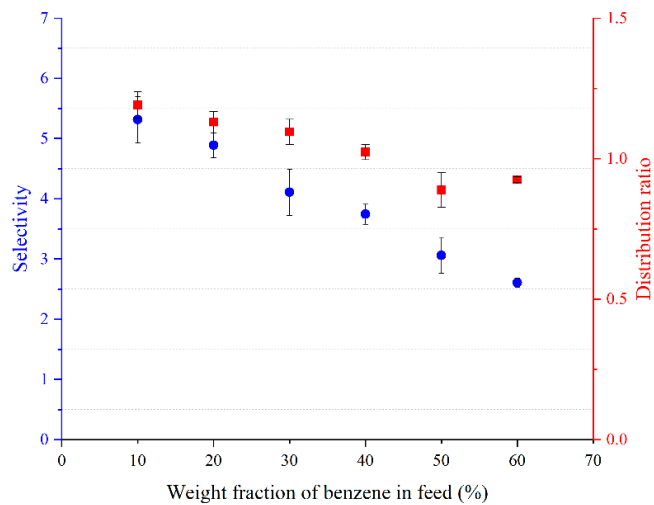


Figure 7. Variation of the distribution ratio and selectivity with benzene weight fraction in the feed for [Benzene (1) + Cyclohexane (2) + TBPB:PTSA (1:1) (3)].

The Othmer-Tobias (Equation (4)) [45] and Hand correlations (Equation (5)) [46] were employed to all ternary systems in order to determine the reliability of the experimental LLE data:

$$\ln\left(\frac{1-w''_{\text{cyc}}}{w''_{\text{cyc}}}\right) = a + b \ln\left(\frac{1-w'_{\text{ES}}}{w'_{\text{ES}}}\right) \quad (4)$$

$$\ln\left(\frac{w''_{\text{Ben}}}{w''_{\text{cyc}}}\right) = c + d \ln\left(\frac{w'_{\text{Ben}}}{w'_{\text{ES}}}\right) \quad (5)$$

where w_{cyc} , w_{ES} , and w_{Ben} denote the concentrations of cyclohexane, ES, and benzene, respectively, a and b refer to the fitting parameters of the Othmer-Tobias correlation, c and d are the fitting parameters of the Hand correlation, and superscripts ' and " refer to the bottom and extract phases, respectively. Table 2 shows the parameters of the Othmer-Tobias and Hand equations. The degree of accuracy of the LLE experimental results is demonstrated by the linearity of the plot (regression coefficient R^2 is close to unity).

Table 2. Parameters of Othmer-Tobias and Hand correlation for ternary systems [benzene + cyclohexane + BTBACl:Ph] and [benzene + cyclohexane + BTBACl:Cre].

ES	Othmer-Tobias			Hand		
	a	b	R ²	c	d	R ²
BTBACl:Ph (1:2)	0.929	1.753	0.982	0.794	1.004	0.998
BTBACl:Cre (1:2)	0.194	1.881	0.998	0.356	0.947	0.994
TBPB:PTSA (1:1)	2.363	1.749	0.974	1.810	1.124	0.988

2.3. Comparison with Other Solvents

The extraction process efficiency can be evaluated by the distribution ratio of benzene and the selectivity of ES. In Figures 8 and 9, the values from this work are compared with some previous reports using different types of extraction solvents, namely organic solvents [47,48], ILs [41,49–51], and ESSs [26]. Sulfolane was used as a benchmark that represents the extractive performance of organic solvents used in the industry. In addition, organic solvents with high selectivity (ethylene glycol, EG) and distribution ratio (dimethylformamide, DMF) were also used for comparison [47]. The full data of both plots and their corresponding ternary molar compositons are summarized in Table S9 of the Supporting Information.

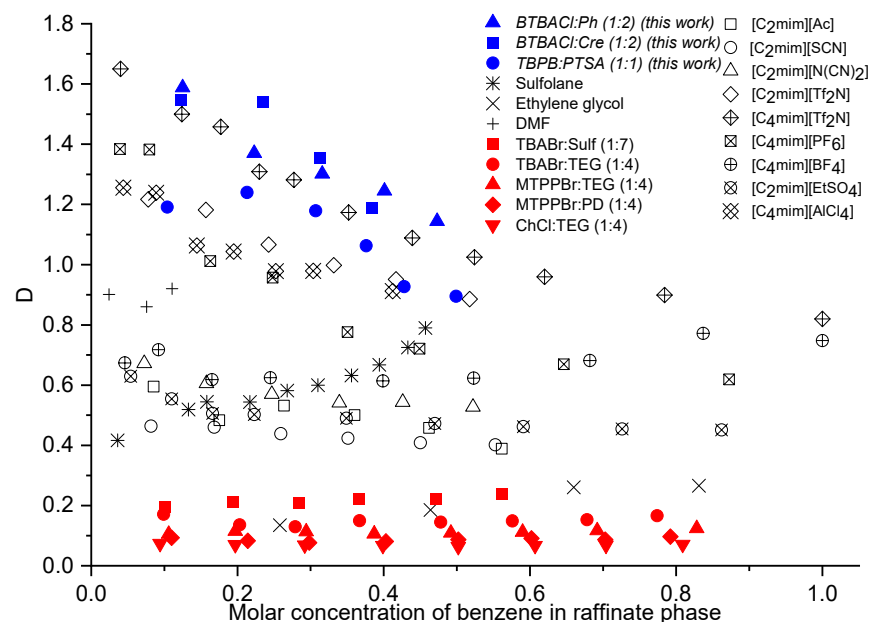


Figure 8. Distribution ratio of organic solvents, ILs, and ESSs for the extractive separation of benzene and cyclohexane.

As can be seen in Figure 8, BTBACl:Ph (1:2) and BTBACl:Cre (1:2) demonstrated the highest benzene distribution ratio compared to other solvents, regardless of the type of solvent, i.e., ESSs, ILs, or conventional solvents. For instance, comparing only the perspective of ESS, when the molar concentration of benzene was around 0.1, the benzene distribution ratio was on the order of BTBACl:Ph > BTBACl:Cre > TBPB:PTSA (1:1) > TBABr:Sulf (1:7) > TBABr: TEG (1:4) > MTPPBr: TEG (1:4) > MTPPBr: PD (1:4) > ChCl: TEG (1:4). This demonstrates the potential of the three ESSs as green solvent alternatives for the separation of benzene and cyclohexane. As for the selectivity depicted in Figure 9, although all ESSs showed the lowest values, all values were greater than unity, indicating the feasibility of the extraction process. The three ESSs also showed higher selectivity than the common organic solvent DMF. Based on the values of benzene distribution ratio and the selectivity, it can be observed that the performance of ESSs to separate the mixture of benzene and cyclohexane

was generally lower than those given by ILs. Nonetheless, this finding does not disregard the feasibility of using ESs for such separation as their experimental selectivity values were higher than unity, indicating the possibility of the extraction process. Furthermore, ESs can also be regenerated and recycled back into the feed stream after the extracted benzene and cyclohexane are removed by anti-solvent extraction or by distillation. In the perspective of extractive separation performance, it can be concluded that ILs are more superior; however, ESs offer remarkable advantages in another perspectives, i.e., cheaper, greener, and easier to prepare than ILs.

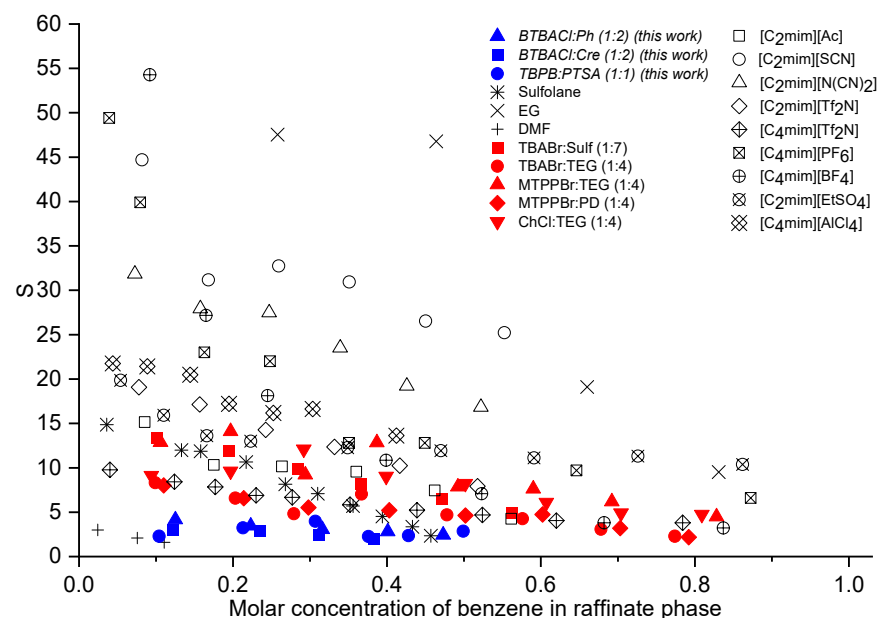


Figure 9. Selectivity of organic solvents, ILs, and ESs for the extractive separation of benzene and cyclohexane.

3. Materials and Methods

3.1. Molecular Geometry Optimization

The geometry optimization of the species involved was conducted using the TMole-X programme package. After the chemical structure of the target molecule was drawn, the geometry optimization was performed at the Hartree-Fock level and the 6-31G* basis set. The .cosmo file was then generated by a single-point calculation using DFT with Becke-Perdew and the Triple- ζ Zeta Valence Potential (TZVP) basis set. Finally, the COSMOthermX programme was used to import the .cosmo files with the parameterization of BP_TZVP_C30_1301.ctd.

3.2. List of ESs for COSMO-RS Screening

The COSMO-RS screening was performed by collecting 20 ESs with aromatic structure from the literature in addition to three new ESs proposed in this work. The studied ESs are shown in Table 3.

Table 3. List of ESs screened in this work using COSMO-RS with their abbreviations.

No	HBA	HBD	Ratio	Abbreviation	Ref.
1	Choline chloride	Benzoic acid	1:1	ChCl:BZA (1:1)	[52–54]
2	Choline chloride	Benzamide	1:2	ChCl:BZM (1:2)	[55]
3	Choline chloride	p-toluenesulfonic acid	1:2	ChCl:PTSA (1:2)	[56]
4	Tetrabutylammonium chloride	p-toluenesulfonic acid	1:2	TBACl:PTSA (1:2)	[56]
5	Tetrabutylammonium bromide	p-toluenesulfonic acid	1:2	TBABr:PTSA (1:2)	[56]
6	Tetraethylammonium chloride	p-toluenesulfonic acid	1:2	TEACl:PTSA (1:2)	[56]

Table 3. Cont.

No	HBA	HBD	Ratio	Abbreviation	Ref.
7	Tetraethylammonium bromide	p-toluenesulfonic acid	1:2	TEABr:PTSA (1:2)	[56]
8	Choline chloride	p-aminosalicylic acid	1:2	ChCl:PAS (1:2)	[56]
9	Trimethylglycine	Benzoic acid	1:1.5	TMGly:BZA (1:1.5)	[57]
10	Trimethylglycine	Salicylic acid	1:1.5	TMGly:SA (1:1.5)	[57]
11	Trimethylglycine	4-chlorobenzoic acid	1:1.5	TMGly:4-CBZ (1:1.5)	[57]
12	Trimethylglycine	3-chlorobenzoic acid	1:1.5	TMGly:3-CBZ (1:1.5)	[57]
13	Trimethylglycine	2-chlorobenzoic acid	1:1.5	TMGly:2-CBZ (1:1.5)	[57]
14	Trimethylglycine	2-furoic acid	1:2	TMGly:2-FA (1:2)	[57]
15	Benzyltrimethylammonium chloride	p-toluenesulfonic acid	3:7	BTMACl:PTSA (3:7)	[58]
16	Benzyltrimethylammonium chloride	Oxalic acid	1:1	BTMACl:OA (1:1)	[58]
17	Benzyltrimethylammonium chloride	Citric acid	1:1	BTMACl:CA (1:1)	[58]
18	N,N-diethylenethanolammonium Cl	p-toluenesulfonic acid	1:3	DEEACl:PTSA (1:3)	[59]
19	Allyltriphenylphosphonium Br	p-toluenesulfonic acid	1:3	ATPPBr:PTSA (1:3)	[60]
20	Choline chloride	p-toluenesulfonic acid	1:2	ChCl:PTSA (1:2)	[61]
21	Benzyltributylammonium chloride	Phenol	1:2	BTBACl:Ph (1:2)	*
22	Benzyltributylammonium chloride	m-Cresol	1:2	BTBACl:Cre (1:2)	*
23	Tetrabutylphosphonium bromide	p-toluenesulfonic acid	1:1	TBPB:PTSA (1:1)	*

* This work.

3.3. ES Representation in COSMOtherm-X

Since a single ES is composed of more than one molecule, employing its representation method in the COSMOtherm-X programme is crucial. ES representation follows the same approach as for ILs, which can be selected from three approaches: (i) the metafile, (ii) the ion-pair, and (iii) the electroneutral. For ILs, the electroneutral approach was usually chosen because it is the most suitable and closest to the actual nature of ILs, where ions are treated as two different compounds in an equimolar mixture. Similarly, this approach was adopted in this study to represent ESs in COSMO-RS based on the molar composition of their constituents (salt cation, salt anion, and hydrogen bond donor (HBD)). The mathematical adaptation has been described in detail in our previous work [35–37].

3.4. Selectivity, Capacity, and Performance Index

The activity coefficient at infinite dilution γ^∞ can be adopted to evaluate the maximum capacity and selectivity of targeted ESs. The value of γ^∞ describes the solute–solvent interactions at an infinitesimal concentration of the solute. In other words, the interaction is evaluated at the far-reaching concentration of the solvent as the concentration of the solute approaches zero. Since γ^∞ accounts only for the IL–solute interaction behaviour and does not reflect the exact extraction ability, it can be further used for calculating the selectivity (S^∞) and capacity (C^∞) of an ES at infinite dilution. S^∞ defines the ability of an ES to interact more with either one of the compounds, and less with another. Therefore, in this case, the selectivity of an ES towards benzene in comparison with cyclohexane ($S_{B,C}^\infty$) can be expressed in terms of the ratio of the activity coefficient for cyclohexane to benzene. This means an ES with high selectivity towards benzene has a high value of γ_C^∞ and a low value of γ_B^∞ .

$$S_{B,C}^\infty = \frac{\gamma_C^\infty}{\gamma_B^\infty} \quad (6)$$

In addition, the amount of an ES required for the extraction process can also be qualitatively determined from the value of C^∞ . The capacity of an ES for benzene (C_B^∞) indicates the maximum amount of benzene that can be dissolved in the ES, which can be calculated with the inverse of the activity coefficient for benzene:

$$C_B^\infty = \frac{1}{\gamma_B^\infty} \quad (7)$$

The final parameter for evaluating the solvent feature in this extraction process is the performance index (PI). It combines both features of capacity and selectivity for estimating the overall performance of an ES. The PI is simply expressed as the product of $S_{B,C}^{\infty}$ and C_B^{∞} :

$$\text{PI} = S_{B,C}^{\infty} \times C_B^{\infty} \quad (8)$$

Table 4 provides a list of the compounds that were used in this work. These chemicals were used without further purification due to their high purity. For each ES, the HBD was combined with the salt in screw cap vials. The vials were then shaken with incubation shakers. Shaking was performed at a speed of 200 rpm and a temperature of 100 °C until a clear liquid was obtained.

Table 4. List of chemicals used in the experimental work.

Chemical	Formula	Purity (wt%)	Supplier	Country
Benzene	C ₆ H ₆	99.5	Panreac	Spain
Cyclohexane	C ₆ H ₁₂	99.5	Analar	England
BTBACl	C ₆ H ₅ CH ₂ N(Cl)(CH ₂ CH ₂ CH ₂ CH ₃) ₃	97	Aldrich	Netherland
Phenol	C ₆ H ₅ O	99.5	VWR International	Belgium
m-Cresol	C ₇ H ₈ O	99	Scharlau	Spain
TBPB	(CH ₃ CH ₂ CH ₂ CH ₂) ₄ P(Br)	98	Aldrich	China
PTSA	C ₇ H ₈ O ₃ S	98.5	Sigma-Aldrich	Japan
Deuterated Chloroform	CDCl ₃	99.8	Sigma-Aldrich	German
Acetonitrile	C ₂ H ₃ N	99.9	VWR International	England

The structures of the studied chemicals are presented in Table S2.

3.5. Liquid–Liquid Equilibria (LLE) Measurements

The LLE data of the ternary mixtures [benzene + cyclohexane + ES] were measured experimentally at 298.15 K. Three ESs were selected for the measurement of experimental LLE data, namely BTBACl:Ph (1:2), BTBACl:Cre (1:2), and TBPB:PTSA (1:1). These ESs were selected mainly because of their liquid nature at room temperature. The desired quantities of ES, benzene, and cyclohexane were mixed in tightly sealed plastic vials within their immiscible concentration range to perform LLE experiments and to achieve tie lines for each system. The feed mixture was obtained by mixing the weighed chemicals with an analytical balance (± 0.0001 g). The vials were then placed in a shaking incubator to control the shaking rate at 200 RPM and the temperature at 298.15 K. The mixture was stirred for 4 h to ensure adequate mixing between the two layers, i.e., extract and raffinate. The vials were then left to rest in the incubator for 12 h to ensure that the equilibrium state was fully reached. Once equilibrium was reached, samples were collected from both layers and analyzed by gas chromatography (GC).

To obtain tie lines, a Trace GC ultra (from Thermo Scientific) was used to determine the compositions of the ES phase and the extract phase (hydrocarbon-rich layer). The chromatograph was equipped with an Rtx-1 column (30 m \times 0.25 mm \times 0.25 μ m) and a flame ionization detector (FID). The temperature ramp of the GC was set to 358.2 K at a rate of 10 K/min. The temperatures for injection and FID were maintained at 584 K. The column oven was maintained at 308.2 K for 2 min. Helium at a constant flow rate of 30 mL/min was used as the carrier gas. A split ratio of 16 was considered with an injection volume of 0.3 μ L. Acetonitrile was used as a diluent. Using this method, the compositions of benzene and cyclohexane in each layer were measured and the corresponding compositions of ES in each layer were determined by mass balance calculations. ES was considered as a single pseudo-component to calculate mole fractions, with a mixture containing benzene and cyclohexane. A calibration curve for benzene and cyclohexane was constructed to measure the composition. Each measurement was tripled by GC and the molar composition was estimated to be ± 0.009 . To confirm the absence of ES in the hydrocarbon-rich phase, ¹H NMR was performed. A JEOL RESPONANCE spectrometer (ECX-500 II) was used to record the ¹H NMR spectra at 298.15 K and CDCl₃ was used as solvent.

In addition, Fourier transform infrared (FTIR) analysis was performed to confirm the structure of the ESs. For example, Figure S4 shows that in pure PTSA, the peaks representing the symmetric and asymmetric stretching of SO_3 in the range of 2800–1800 cm^{-1} disappeared after the formation of ES. It can be seen that the hydrogen bonding occurred between PTSA and TBPB instead of between PTSA and H_2O . Similar phenomena of disappearance of the SO_3 peak to form a bond for the components of ES were also previously [62,63] reported in PTSA-based ESs, e.g., PTSA:tetrabutylphosphonium chloride (1:1), PTSA:tetrabutylammonium chloride (1:1), and PTSA:ChCl (1:1). Hydrogen bond formation between BTBACl and m-cresol is the driving force behind the synthesis of ES. As shown in Figure S5, absorptions associated with O-H at 3336 cm^{-1} were observed in the FTIR spectra of pure m-cresol. The O-H vibration of m-cresol shifted to 3172 cm^{-1} in the FTIR of ES. These shifts might have been caused by the transfer of an electron from an oxygen atom to the hydrogen bond, leading to a decrease in the force constant [64,65]. When the ES was formed, the shift in O-H vibrations indicated hydrogen bonding between BTBACl and m-cresol. In Figure S6, FTIR analysis of pure phenol showed the formation of O-H (3243 cm^{-1}), C=C (1475 and 1596 cm^{-1}), and C-O (1233 cm^{-1}). In the FTIR spectrum of ES, all the peaks of phenol were approximately in the same range as the peaks of pure phenol, except for the peak associated with the O-H bond. In the ES, the O-H vibrations of pure phenol (3243 cm^{-1}) shifted to 3169 cm^{-1} . This phenomenon may indicate the sharing of oxygen atom electrons to form the hydrogen bond between phenol and BTBACl during the formation of ES. Similar behavior was observed by Mehran et al. [66] for phenol-based ESs.

4. Conclusions

The potential of ESs containing constituents with an aromatic structure for extractive separation of benzene–cyclohexane mixture was explored in this work. COSMO-RS was used to preselect the ESs. From the 23 candidates screened, 3 ESs were selected for experimental validation, where their extractive performances to separate benzene and cyclohexane mixture were studied through liquid–liquid extraction process. Ternary LLE data were acquired for the three ESs, i.e., BTBACl:Ph (1:2)/BTBACl:Cre (1:2)/TBPB:PTSA (1:1) + benzene + cyclohexane at 25 °C and 101.325 kPa. It was found that BTBACl:Cres (1:2) and BTBACl:Ph (1:2) show high distribution compared to other solvents, i.e., conventional solvents, ILs, and other ESs in previous works.

Supplementary Materials: The following supporting information can be downloaded at: <https://www.mdpi.com/article/10.3390/molecules27134041/s1>, Figure S1: CDCl_3 : (a) pure BTBACl:Ph (1:2) ES; (b) Extract layer. Figure S2: ^1H NMR spectra in CDCl_3 : (a) pure BTBACl:Cre (1:2) ES; (b) Extract layer. Figure S3: ^1H NMR spectra in CDCl_3 : (a) pure TBPB:PTSA (1:1) ES; (b) Extract layer. Figures S4–S6: FTIR analysis of all three ESs and their individual components. Table S1: Some examples of ESs in various fields. Table S2: Structures of the studied chemicals. Tables S3 and S4: Standard deviation (STDEV) on measured solubilities with BTBACl:Ph (1:2) (3) for the top layer and bottom layer. Tables S5 and S6: STDEV on measured solubilities with BTBACl:Cre (1:2) (3) for the top layer and bottom layer. Tables S7 and S8: Standard deviation (STDEV) on measured solubilities with TBPB:PTSA (1:1) (3) for the top layer and bottom layer. Table S9: Molar ternary compositions, benzene distribution ratio (DBz) and solvent selectivity (S) from previous works involving organic solvents, ILs, and ESs. x_1 , x_2 , and x_3 represents the molar composition of benzene, cyclohexane, and solvents, respectively. References [67–98] are cited in the supplementary materials.

Author Contributions: Conceptualization, M.K.H.-K. and M.Z.M.S.; methodology, M.K.H.-K. and M.Z.M.S.; software, M.K.H.-K. and M.Z.M.S.; validation, I.W., A.A. and S.M.; formal analysis, M.Z.M.S., I.W. and S.M.; investigation, M.K.H.-K.; resources, M.Z.M.S., I.W. and S.M.; data curation, M.Z.M.S., I.W. and S.M.; writing—original draft preparation, M.Z.M.S. and I.W.; writing—review and editing, M.K.H.-K., M.Z.M.S., I.W. and A.A.; visualization, M.Z.M.S. and S.M.; supervision, M.K.H.-K.; project administration, M.K.H.-K.; funding acquisition, M.K.H.-K. All authors have read and agreed to the published version of the manuscript.

Funding: This research was funded by the Researchers Supporting Project number (RSP-2021/361), King Saud University, Riyadh, Saudi Arabia.

Institutional Review Board Statement: Not applicable.

Informed Consent Statement: Not applicable.

Conflicts of Interest: The authors declare no conflict of interest.

Sample Availability: Samples of the compounds are not available from the authors.

References

1. Weissermel, K.; Arpe, H.J.; Lindley, C.R.; Hawkins, S. *Industrial Organic Chemistry*; Wiley-VCH: Weinheim, Germany, 2003.
2. Rydberg, J. *Solvent Extraction Principles and Practice, Revised and Expanded*; CRC Press: New York, NY, USA, 2004.
3. Stichlmair, J.G.; Fair, J.R. *Distillation: Principles and Practices*; Wiley: New York, NY, USA, 1998.
4. Lubben, M.J.; Canales, R.I.; Lyu, Y.; Held, C.; Gonzalez-Miquel, M.; Stadtherr, M.A.; Brennecke, J.F. Promising Thiolanium Ionic Liquid for Extraction of Aromatics from Aliphatics: Experiments and Modeling. *Ind. Eng. Chem. Res.* **2020**, *59*, 15707–15717. [[CrossRef](#)]
5. Delgado-Mellado, N.; Ovejero-Perez, A.; Navarro, P.; Larriba, M.; Ayuso, M.; García, J.; Rodríguez, F. Imidazolium and pyridinium-based ionic liquids for the cyclohexane/cyclohexene separation by liquid-liquid extraction. *J. Chem. Thermodyn.* **2019**, *131*, 340–346. [[CrossRef](#)]
6. Ayuso, M.; Navarro, P.; Palma, A.M.; Larriba, M.; Delgado-Mellado, N.; García, J.; Rodríguez, F.; Coutinho, J.A.; Carvalho, P.J. Toward modeling the aromatic/aliphatic separation by extractive distillation with tricyanomethane-based ionic liquids using CPA EoS. *Ind. Eng. Chem. Res.* **2019**, *58*, 19681–19692. [[CrossRef](#)]
7. Capela, E.V.; Quental, M.V.; Domingues, P.; Coutinho, J.A.; Freire, M.G. Effective separation of aromatic and aliphatic amino acid mixtures using ionic-liquid-based aqueous biphasic systems. *Green Chem.* **2017**, *19*, 1850–1854. [[CrossRef](#)]
8. Hashim, M.; Zulhaziman, M.; Salleh, M.; Ali, E.; Hadj-Kali, M.K. Selective extraction of benzene from benzene–cyclohexane mixture using 1-ethyl-3-methylimidazolium tetrafluoroborate ionic liquid. *AIP Conf. Proc.* **2019**, *2124*, 020028.
9. Zhou, T.; Wang, Z.; Chen, L.; Ye, Y.; Qi, Z.; Freund, H.; Sundmacher, K. Evaluation of the ionic liquids 1-alkyl-3-methylimidazolium hexafluorophosphate as a solvent for the extraction of benzene from cyclohexane: (Liquid+liquid) equilibria. *J. Chem. Thermodyn.* **2012**, *48*, 145–149. [[CrossRef](#)]
10. Gómez, E.; Domínguez, I.; Calvar, N.; Domínguez, Á. Separation of benzene from alkanes by solvent extraction with 1-ethylpyridinium ethylsulfate ionic liquid. *J. Chem. Thermodyn.* **2010**, *42*, 1234–1239. [[CrossRef](#)]
11. Gómez, E.; Domínguez, I.; Gonzalez, B.; Domínguez, A. Liquid–liquid equilibria of the ternary systems of alkane+aromatic+1-ethylpyridinium ethylsulfate ionic liquid at T = (283.15 and 298.15) K. *J. Chem. Eng. Data* **2010**, *55*, 5169–5175. [[CrossRef](#)]
12. Zhao, D.; Liao, Y.; Zhang, Z. Toxicity of ionic liquids. *Clean Soil Air Water* **2007**, *35*, 42–48. [[CrossRef](#)]
13. Warrag, S.E.; Peters, C.J.; Kroon, M.C. Deep eutectic solvents for highly efficient separations in oil and gas industries. *Curr. Opin. Green Sustain. Chem.* **2017**, *5*, 55–60. [[CrossRef](#)]
14. Bernasconi, R.; Panzeri, G.; Accogli, A.; Liberale, F.; Nobili, L.; Magagnin, L. Electrodeposition from deep eutectic solvents. *Intech. Prog. Dev. Lon. Liq.* **2017**, 235–261. [[CrossRef](#)]
15. Abo-Hamad, A.; Hayyan, M.; AlSaadi, M.A.; Hashim, M.A. Potential applications of deep eutectic solvents in nanotechnology. *Chem. Eng. J.* **2015**, *273*, 551–567. [[CrossRef](#)]
16. Cunha, S.C.; Fernandes, J.O. Extraction techniques with deep eutectic solvents. *TrAC Trends Anal. Chem.* **2018**, *105*, 225–239. [[CrossRef](#)]
17. Li, X.; Row, K.H. Development of deep eutectic solvents applied in extraction and separation. *J. Sep. Sci.* **2016**, *39*, 3505–3520. [[CrossRef](#)] [[PubMed](#)]
18. Boldrini, C.L.; Quivelli, A.F.; Manfredi, N.; Capriati, V.; Abbotto, A. Deep Eutectic Solvents in Solar Energy Technologies. *Molecules* **2022**, *27*, 709. [[CrossRef](#)] [[PubMed](#)]
19. Perna, F.M.; Vitale, P.; Capriati, V. Deep eutectic solvents and their applications as green solvents. *Curr. Opin. Green Sustain. Chem.* **2020**, *21*, 27–33. [[CrossRef](#)]
20. Milano, F.; Giotta, L.; Guascito, M.R.; Agostiano, A.; Sbendorio, S.; Valli, L.; Perna, F.M.; Cicco, L.; Trotta, M.; Capriati, V. Functional enzymes in nonaqueous environment: The case of photosynthetic reaction centers in deep eutectic solvents. *ACS Sustain. Chem. Eng.* **2017**, *5*, 7768–7776. [[CrossRef](#)]
21. Brett, C.M. Deep eutectic solvents and applications in electrochemical sensing. *Curr. Opin. Electrochem.* **2018**, *10*, 143–148. [[CrossRef](#)]
22. Tang, B.; Row, K.H. Recent developments in deep eutectic solvents in chemical sciences. *Mon. Chem. Chem. Mon.* **2013**, *144*, 1427–1454. [[CrossRef](#)]
23. Zhang, Q.; Vigier, K.D.O.; Royer, S.; Jerome, F. Deep eutectic solvents: Syntheses, properties and applications. *Chem. Soc. Rev.* **2012**, *41*, 7108–7146. [[CrossRef](#)]
24. Kalhor, P.; Ghandi, K. Deep eutectic solvents for pretreatment, extraction, and catalysis of biomass and food waste. *Molecules* **2019**, *24*, 4012. [[CrossRef](#)] [[PubMed](#)]
25. Smith, E.L.; Abbott, A.P.; Ryder, K.S. Deep eutectic solvents (DESs) and their applications. *Chem. Rev.* **2014**, *114*, 11060–11082. [[CrossRef](#)] [[PubMed](#)]

26. Salleh, Z.; Wazeer, I.; Mulyono, S.; El-blidi, L.; Hashim, M.A.; Hadj-Kali, M.K. Efficient removal of benzene from cyclohexane–benzene mixtures using deep eutectic solvents–COSMO-RS screening and experimental validation. *J. Chem. Thermodyn.* **2017**, *104*, 33–44. [[CrossRef](#)]
27. Ma, S.; Li, J.; Li, L.; Shang, X.; Liu, S.; Xue, C.; Sun, L. Liquid–liquid extraction of benzene and cyclohexane using sulfolane-based low transition temperature mixtures as solvents: Experiments and simulation. *Energy Fuels* **2018**, *32*, 8006–8015. [[CrossRef](#)]
28. García, S.; Larriba, M.; García, J.; Torrecilla, J.S.; Rodríguez, F. Liquid–liquid extraction of toluene from n-heptane using binary mixtures of N-butylpyridinium tetrafluoroborate and N-butylpyridinium bis (trifluoromethylsulfonyl) imide ionic liquids. *Chem. Eng. J.* **2012**, *180*, 210–215. [[CrossRef](#)]
29. Salleh, M.Z.M.; Hadj-Kali, M.; Wazeer, I.; Ali, E.; Hashim, M.A. Extractive separation of benzene and cyclohexane using binary mixtures of ionic liquids. *J. Mol. Liq.* **2019**, *285*, 716–726. [[CrossRef](#)]
30. Larriba, M.; de Riva, J.; Navarro, P.; Moreno, D.; Delgado-Mellado, N.; García, J.; Ferro, V.R.; Rodríguez, F.; Palomar, J. COSMO-based/Aspen Plus process simulation of the aromatic extraction from pyrolysis gasoline using the {[4empty][NTf₂]+[emim][DCA]} ionic liquid mixture. *Sep. Purif. Technol.* **2018**, *190*, 211–227. [[CrossRef](#)]
31. Larriba, M.; Navarro, P.; González, E.J.; García, J.; Rodríguez, F. Separation of BTEX from a naphtha feed to ethylene crackers using a binary mixture of [4empty][Tf₂N] and [emim][DCA] ionic liquids. *Sep. Purif. Technol.* **2015**, *144*, 54–62. [[CrossRef](#)]
32. Larriba, M.; Navarro, P.; García, J.; Rodríguez, F. Liquid–Liquid Extraction of Toluene from n-Alkanes using {[4empty][Tf₂N]+[emim][DCA]} Ionic Liquid Mixtures. *J. Chem. Eng. Data* **2014**, *59*, 1692–1699. [[CrossRef](#)]
33. Klamt, A. Conductor-like screening model for real solvents: A new approach to the quantitative calculation of solvation phenomena. *J. Phys. Chem.* **1995**, *99*, 2224–2235. [[CrossRef](#)]
34. Klamt, A.; Eckert, F. COSMO-RS: A novel and efficient method for the a priori prediction of thermophysical data of liquids. *Fluid Phase Equilib.* **2000**, *172*, 43–72. [[CrossRef](#)]
35. Hizaddin, H.F.; Sarwono, M.; Hashim, M.A.; Alnashef, I.M.; Hadj-Kali, M.K. Coupling the capabilities of different complexing agents into deep eutectic solvents to enhance the separation of aromatics from aliphatics. *J. Chem. Thermodyn.* **2015**, *84*, 67–75. [[CrossRef](#)]
36. Mulyono, S.; Hizaddin, H.F.; Alnashef, I.M.; Hashim, M.A.; Fakieha, A.H.; Hadj-Kali, M.K. Separation of BTEX aromatics from n-octane using a (tetrabutylammonium bromide+sulfolane) deep eutectic solvent—experiments and COSMO-RS prediction. *RSC Adv.* **2014**, *4*, 17597–17606. [[CrossRef](#)]
37. Hizaddin, H.F.; Ramalingam, A.; Hashim, M.A.; Hadj-Kali, M.K. Evaluating the performance of deep eutectic solvents for use in extractive denitrification of liquid fuels by the conductor-like screening model for real solvents. *J. Chem. Eng. Data* **2014**, *59*, 3470–3487. [[CrossRef](#)]
38. Anantharaj, R.; Banerjee, T. Aromatic sulfur-nitrogen extraction using ionic liquids: Experiments and predictions using an a priori model. *AIChE J.* **2013**, *59*, 4806–4815. [[CrossRef](#)]
39. Anantharaj, R.; Banerjee, T. COSMO-RS based predictions for the desulphurization of diesel oil using ionic liquids: Effect of cation and anion combination. *Fuel Process. Technol.* **2011**, *92*, 39–52. [[CrossRef](#)]
40. Wilfred, C.D.; Man, Z.; Chan, Z.P. Predicting methods for sulfur removal from model oils using COSMO-RS and partition coefficient. *Chem. Eng. Sci.* **2013**, *102*, 373–377. [[CrossRef](#)]
41. Zhou, T.; Wang, Z.; Ye, Y.; Chen, L.; Xu, J.; Qi, Z. Deep separation of benzene from cyclohexane by liquid extraction using ionic liquids as the solvent. *Ind. Eng. Chem. Res.* **2012**, *51*, 5559–5564. [[CrossRef](#)]
42. Gonfa, G.; Bustam, M.A.; Murugesan, T.; Man, Z.; Mutalib, M. Thiocyanate based task-specific ionic liquids for separation of benzene and cyclohexane. *Chem. Eng.* **2013**, *32*, 1939–1944.
43. Lyu, Z.; Zhou, T.; Chen, L.; Ye, Y.; Sundmacher, K.; Qi, Z. Simulation based ionic liquid screening for benzene–cyclohexane extractive separation. *Chem. Eng. Sci.* **2014**, *113*, 45–53. [[CrossRef](#)]
44. Rodriguez, N.R.; Requejo, P.F.; Kroon, M.C. Aliphatic–aromatic separation using deep eutectic solvents as extracting agents. *Ind. Eng. Chem. Res.* **2015**, *54*, 11404–11412. [[CrossRef](#)]
45. Othmer, D.; Tobias, P. Liquid–liquid extraction data—the line correlation. *Ind. Eng. Chem.* **1942**, *34*, 693–696. [[CrossRef](#)]
46. Hand, D.B. Dineric distribution. *J. Phys. Chem.* **1930**, *34*, 1961–2000. [[CrossRef](#)]
47. Aspi, K.K.; Surana, N.M.; Ethirajulu, K.; Vennila, V. Liquid–Liquid Equilibria for the Cyclohexane+Benzene+Dimethylformamide +Ethylene Glycol System. *J. Chem. Eng. Data* **1998**, *43*, 925–927. [[CrossRef](#)]
48. Chen, J.; Li, Z.; Duan, L. Liquid–Liquid Equilibria of Ternary and Quaternary Systems Including Cyclohexane, 1-Heptene, Benzene, Toluene, and Sulfolane at 298.15 K. *J. Chem. Eng. Data* **2000**, *45*, 689–692. [[CrossRef](#)]
49. Calvar, N.; Domínguez, I.; Gómez, E.; Domínguez, Á. Separation of binary mixtures aromatic+aliphatic using ionic liquids: Influence of the structure of the ionic liquid, aromatic and aliphatic. *Chem. Eng. J.* **2011**, *175*, 213–221. [[CrossRef](#)]
50. González, E.J.; Calvar, N.; González, B.; Domínguez, Á. Liquid Extraction of Benzene from Its Mixtures Using 1-Ethyl-3-methylimidazolium Ethylsulfate as a Solvent. *J. Chem. Eng. Data* **2010**, *55*, 4931–4936. [[CrossRef](#)]
51. Sakal, S.A.; Shen, C.; Li, C.-X. (Liquid+liquid) equilibria of {benzene+cyclohexane+two ionic liquids} at different temperature and atmospheric pressure. *J. Chem. Thermodyn.* **2012**, *49*, 81–86. [[CrossRef](#)]
52. Muthuraman, G.; Teng, T.T.; Leh, C.P.; Norli, I. Extraction and recovery of methylene blue from industrial wastewater using benzoic acid as an extractant. *J. Hazard. Mater.* **2009**, *163*, 363–369. [[CrossRef](#)]

53. Cheng, W.T.; Feng, S.; Cui, X.Q.; Cheng, F.Q. Solubility of Benzoic Acid in Ethanol, Benzene, Acetic Acid and Ethyl Acetate from 291.69 to 356.27 K. *Adv. Mater. Res.* **2012**, *518–523*, 3975–3979. [[CrossRef](#)]
54. Abbott, A.P.; Boothby, D.; Capper, G.; Davies, D.L.; Rasheed, R.K. Deep Eutectic Solvents Formed between Choline Chloride and Carboxylic Acids: Versatile Alternatives to Ionic Liquids. *J. Am. Chem. Soc.* **2004**, *126*, 9142–9147. [[CrossRef](#)] [[PubMed](#)]
55. Abbott, A.P.; Capper, G.; Davies, D.L.; Rasheed, R.K.; Tambyrajah, V. Novel solvent properties of choline chloride/urea mixtures. *Chem. Commun.* **2003**, *70–71*. [[CrossRef](#)] [[PubMed](#)]
56. Yin, J.; Wang, J.; Li, Z.; Li, D.; Yang, G.; Cui, Y.; Wang, A.; Li, C. Deep desulfurization of fuels based on an oxidation/extraction process with acidic deep eutectic solvents. *Green Chem.* **2015**, *17*, 4552–4559. [[CrossRef](#)]
57. Cardellini, F.; Tiecco, M.; Germani, R.; Cardinali, G.; Corte, L.; Roscini, L.; Spreti, N. Novel zwitterionic deep eutectic solvents from trimethylglycine and carboxylic acids: Characterization of their properties and their toxicity. *RSC Adv.* **2014**, *4*, 55990–56002. [[CrossRef](#)]
58. Taysun, M.B.; Sert, E.; Atalay, F.S. Physical properties of benzyl tri-methyl ammonium chloride based deep eutectic solvents and employment as catalyst. *J. Mol. Liq.* **2016**, *223*, 845–852. [[CrossRef](#)]
59. Hayyan, A.; Hashim, M.A.; Hayyan, M.; Mjalli, F.S.; AlNashef, I.M. A novel ammonium based eutectic solvent for the treatment of free fatty acid and synthesis of biodiesel fuel. *Ind. Crops Prod.* **2013**, *46*, 392–398. [[CrossRef](#)]
60. Hayyan, A.; Ali Hashim, M.; Mjalli, F.S.; Hayyan, M.; AlNashef, I.M. A novel phosphonium-based deep eutectic catalyst for biodiesel production from industrial low grade crude palm oil. *Chem. Eng. Sci.* **2013**, *92*, 81–88. [[CrossRef](#)]
61. Martins, M.A.P.; Pavaglio, G.C.; Munchen, T.S.; Meyer, A.R.; Moreira, D.N.; Rodrigues, L.V.; Frizzo, C.P.; Zanatta, N.; Bonacorso, H.G.; Melo, P.A.; et al. Deep eutectic solvent mediated synthesis of thiomethyltriazolo[1,5-a]pyrimidines. *J. Mol. Liq.* **2016**, *223*, 934–938. [[CrossRef](#)]
62. Kamarudin, A.F.; Hizaddin, H.F.; El-Blidi, L.; Ali, E.; Hashim, M.A.; Hadj-Kali, M.K. Performance of p-Toluenesulfonic Acid-Based Deep Eutectic Solvent in Denitrogenation: Computational Screening and Experimental Validation. *Molecules* **2020**, *25*, 5093. [[CrossRef](#)]
63. Rodriguez Rodriguez, N.; Machiels, L.; Binnemans, K. *p*-Toluenesulfonic acid-based deep-eutectic solvents for solubilizing metal oxides. *ACS Sustain. Chem. Eng.* **2019**, *7*, 3940–3948. [[CrossRef](#)]
64. Guo, W.; Hou, Y.; Wu, W.; Ren, S.; Tian, S.; Marsh, K.N. Separation of phenol from model oils with quaternary ammonium salts via forming deep eutectic solvents. *Green Chem.* **2013**, *15*, 226–229. [[CrossRef](#)]
65. Babaee, S.; Daneshfar, A. Magnetic deep eutectic solvent-based ultrasound-assisted liquid–liquid microextraction for determination of hexanal and heptanal in edible oils followed by gas chromatography–flame ionization detection. *Anal. Methods* **2018**, *10*, 4162–4169. [[CrossRef](#)]
66. Pourhossein, M.; Heravizadeh, O.R.; Omidi, F.; Khadem, M.; Jamaleddin, S. Ultrasound-Assisted Emulsified Microextraction Based on Deep Eutectic Solvent for Trace Residue Analysis of Metribuzin in Urine Samples. *Methods Objects Chem. Anal.* **2021**, *16*, 153–161. [[CrossRef](#)]
67. Oliveira, F.S.; Pereiro, A.B.; Rebelo, L.P.; Marrucho, I.M. Deep eutectic solvents as extraction media for azeotropic mixtures. *Green Chem.* **2013**, *15*, 1326–1330. [[CrossRef](#)]
68. van Osch, D.J.; Zubeir, L.F.; van den Bruinhorst, A.; Rocha, M.A.; Kroon, M.C. Hydrophobic deep eutectic solvents as water-immiscible extractants. *Green Chem.* **2015**, *17*, 4518–4521. [[CrossRef](#)]
69. Phelps, T.E.; Bhawawet, N.; Jurisson, S.S.; Baker, G.A. Efficient and selective extraction of 99m TcO₄[−] from aqueous media using hydrophobic deep eutectic solvents. *ACS Sustain. Chem. Eng.* **2018**, *6*, 13656–13661. [[CrossRef](#)]
70. Schaeffer, N.; Martins, M.A.; Neves, C.M.; Pinho, S.P.; Coutinho, J.A. Sustainable hydrophobic terpene-based eutectic solvents for the extraction and separation of metals. *Chem. Commun.* **2018**, *54*, 8104–8107. [[CrossRef](#)]
71. Tereshatov, E.; Boltoeva, M.Y.; Folden, C. First evidence of metal transfer into hydrophobic deep eutectic and low-transition-temperature mixtures: Indium extraction from hydrochloric and oxalic acids. *Green Chem.* **2016**, *18*, 4616–4622. [[CrossRef](#)]
72. Almustafa, G.; Sulaiman, R.; Kumar, M.; Adeyemi, I.; Arafat, H.A.; AlNashef, I. Boron extraction from aqueous medium using novel hydrophobic deep eutectic solvents. *Chem. Eng. J.* **2020**, *395*, 125173. [[CrossRef](#)]
73. Zante, G.; Braun, A.; Masmoudi, A.; Barillon, R.; Trebouet, D.; Boltoeva, M. Solvent extraction fractionation of manganese, cobalt, nickel and lithium using ionic liquids and deep eutectic solvents. *Miner. Eng.* **2020**, *156*, 106512. [[CrossRef](#)]
74. Liu, X.; Gao, B.; Jiang, Y.; Ai, N.; Deng, D. Solubilities and thermodynamic properties of carbon dioxide in guaiacol-based deep eutectic solvents. *J. Chem. Eng. Data* **2017**, *62*, 1448–1455. [[CrossRef](#)]
75. Altamash, T.; Nasser, M.S.; Elhamarnah, Y.; Magzoub, M.; Ullah, R.; Qiblawey, H.; Aparicio, S.; Atilhan, M. Gas solubility and rheological behavior study of betaine and alanine based natural deep eutectic solvents (NADES). *J. Mol. Liq.* **2018**, *256*, 286–295. [[CrossRef](#)]
76. Sarmad, S.; Xie, Y.; Mikkola, J.-P.; Ji, X. Screening of deep eutectic solvents (DESs) as green CO₂ sorbents: From solubility to viscosity. *New J. Chem.* **2017**, *41*, 290–301. [[CrossRef](#)]
77. Li, X.; Hou, M.; Han, B.; Wang, X.; Zou, L. Solubility of CO₂ in a choline chloride+ urea eutectic mixture. *J. Chem. Eng. Data* **2008**, *53*, 548–550. [[CrossRef](#)]
78. Leron, R.B.; Li, M.-H. Solubility of carbon dioxide in a choline chloride–ethylene glycol based deep eutectic solvent. *Thermochim. Acta* **2013**, *551*, 14–19. [[CrossRef](#)]

79. Jenkin, G.R.; Al-Bassam, A.Z.; Harris, R.C.; Abbott, A.P.; Smith, D.J.; Holwell, D.A.; Chapman, R.J.; Stanley, C.J. The application of deep eutectic solvent ionic liquids for environmentally-friendly dissolution and recovery of precious metals. *Miner. Eng.* **2016**, *87*, 18–24. [[CrossRef](#)]
80. Abbott, A.P.; Capper, G.; McKenzie, K.J.; Ryder, K.S. Electrodeposition of zinc–tin alloys from deep eutectic solvents based on choline chloride. *J. Electroanal. Chem.* **2007**, *599*, 288–294. [[CrossRef](#)]
81. You, Y.; Gu, C.; Wang, X.; Tu, J. Electrodeposition of Ni–Co alloys from a deep eutectic solvent. *Surf. Coat. Technol.* **2012**, *206*, 3632–3638. [[CrossRef](#)]
82. Malaquias, J.C.; Steichen, M.; Thomassey, M.; Dale, P.J. Electrodeposition of Cu–In alloys from a choline chloride based deep eutectic solvent for photovoltaic applications. *Electrochim. Acta* **2013**, *103*, 15–22. [[CrossRef](#)]
83. Gómez, E.; Cojocaru, P.; Magagnin, L.; Valles, E. Electrodeposition of Co, Sm and SmCo from a deep eutectic solvent. *J. Electroanal. Chem.* **2011**, *658*, 18–24. [[CrossRef](#)]
84. Gu, C.; Tu, J. One-step fabrication of nanostructured Ni film with lotus effect from deep eutectic solvent. *Langmuir* **2011**, *27*, 10132–10140. [[CrossRef](#)] [[PubMed](#)]
85. Whitehead, A.H.; Pötzler, M.; Gollas, B. Zinc electrodeposition from a deep eutectic system containing choline chloride and ethylene glycol. *J. Electrochem. Soc.* **2010**, *157*, D328. [[CrossRef](#)]
86. Abbott, A.P.; Capper, G.; Davies, D.L.; McKenzie, K.J.; Obi, S.U. Solubility of metal oxides in deep eutectic solvents based on choline chloride. *J. Chem. Eng. Data* **2006**, *51*, 1280–1282. [[CrossRef](#)]
87. Raghuwanshi, V.S.; Ochmann, M.; Hoell, A.; Polzer, F.; Rademann, K. Deep eutectic solvents for the self-assembly of gold nanoparticles: A SAXS, UV–Vis, and TEM investigation. *Langmuir* **2014**, *30*, 6038–6046. [[CrossRef](#)]
88. Huang, Y.; Shen, F.; La, J.; Luo, G.; Lai, J.; Liu, C.; Chu, G. Synthesis and characterization of CuCl nanoparticles in deep eutectic solvents. *Part. Sci. Technol.* **2013**, *31*, 81–84. [[CrossRef](#)]
89. Adhikari, L.; Larm, N.E.; Baker, G.A. Argentous deep eutectic solvent approach for scaling up the production of colloidal silver nanocrystals. *ACS Sustain. Chem. Eng.* **2019**, *7*, 11036–11043. [[CrossRef](#)]
90. Hayyan, M.; Mjalli, F.S.; Hashim, M.A.; AlNashef, I.M. A novel technique for separating glycerine from palm oil-based biodiesel using ionic liquids. *Fuel Process. Technol.* **2010**, *91*, 116–120. [[CrossRef](#)]
91. Abbott, A.P.; Cullis, P.M.; Gibson, M.J.; Harris, R.C.; Raven, E. Extraction of glycerol from biodiesel into a eutectic based ionic liquid. *Green Chem.* **2007**, *9*, 868–872. [[CrossRef](#)]
92. Zhao, H.; Baker, G.A.; Holmes, S. New eutectic ionic liquids for lipase activation and enzymatic preparation of biodiesel. *Org. Biomol. Chem.* **2011**, *9*, 1908–1916. [[CrossRef](#)]
93. Zhao, H.; Zhang, C.; Crittle, T.D. Choline-based deep eutectic solvents for enzymatic preparation of biodiesel from soybean oil. *J. Mol. Catal. B Enzym.* **2013**, *85*, 243–247. [[CrossRef](#)]
94. Xu, Q.; Qin, L.Y.; Ji, Y.N.; Leung, P.K.; Su, H.N.; Qiao, F.; Yang, W.W.; Shah, A.A.; Li, H.M. A deep eutectic solvent (DES) electrolyte-based vanadium–iron redox flow battery enabling higher specific capacity and improved thermal stability. *Electrochim. Acta* **2019**, *293*, 426–431. [[CrossRef](#)]
95. Jhong, H.-R.; Wong, D.S.-H.; Wan, C.-C.; Wang, Y.-Y.; Wei, T.-C. A novel deep eutectic solvent-based ionic liquid used as electrolyte for dye-sensitized solar cells. *Electrochim. Commun.* **2009**, *11*, 209–211. [[CrossRef](#)]
96. Boldrini, C.L.; Manfredi, N.; Perna, F.M.; Trifiletti, V.; Capriati, V.; Abbotto, A. Dye-sensitized solar cells that use an aqueous choline chloride-based deep eutectic solvent as effective electrolyte solution. *Energy Technol.* **2017**, *5*, 345–353. [[CrossRef](#)]
97. Bozzini, B.; Busson, B.; Humbert, C.; Mele, C.; Tadjeddine, A. Electrochemical fabrication of nanoporous gold decorated with manganese oxide nanowires from eutectic urea/choline chloride ionic liquid. Part III—Electrodeposition of Au–Mn: A study based on in situ Sum-Frequency Generation and Raman spectroscopies. *Electrochim. Acta* **2016**, *218*, 208–215. [[CrossRef](#)]
98. Lu, Y.-S.; Pan, W.-Y.; Hung, T.-C.; Hsieh, Y.-T. Electrodeposition of silver in a ternary deep eutectic solvent and the electrochemical sensing ability of the Ag-modified electrode for nitrofurazone. *Langmuir* **2020**, *36*, 11358–11365. [[CrossRef](#)]